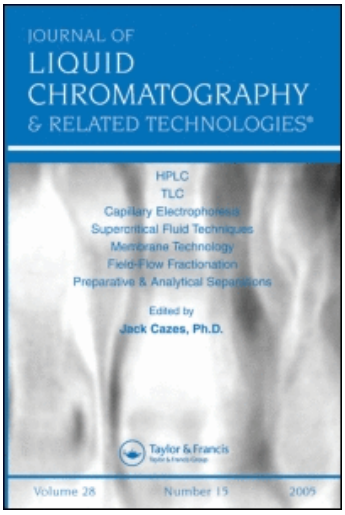

Journal of Liquid Chromatography & Related Technologies
Publication details, including instructions for authors and subscription information:
http://www.informaworld.com/smpp/title~content=t713597273

NEW APPROACH TO MODEL FITTING IN MULTI-DETECTOR GPC

Y. Brun; M. V. Gorenstein; N. Hay

Online publication date: 19 October 2000

To cite this Article Brun, Y. , Gorenstein, M. V. and Hay, N.(2000) 'NEW APPROACH TO MODEL FITTING IN MULTI-DETECTOR GPC', Journal of Liquid Chromatography & Related Technologies, 23: 17, 2615 — 2639
To link to this Article: DOI: 10.1081/JLC-100101822
URL: http://dx.doi.org/10.1081/JLC-100101822

J. LIQ. CHROM. & REL. TECHNOL., 23(17), 2615–2639 (2000)

NEW APPROACH TO MODEL FITTING IN MULTI-DETECTOR GPC

Y. Brun,* M. V. Gorenstein, N. Hay

Waters Corporation
34 Maple Street
Milford, MA 01757, USA

ABSTRACT

The main limitation of multi-detector GPC arises from the nature of detector sensitivities in the tails of a polymer distribution. In the low molecular weight tail of this distribution, molecular weight-sensitive detectors (such as a capillary viscometer or a static laser light-scattering photometer) have low sensitivity while concentration detectors (e.g., differential refractometer) have high sensitivity. This situation is reversed in the high molecular weight tail.

These imbalances in sensitivity raise the question of how best to obtain an estimate of column calibration curves. The question is central to the successful application of the multi-detector GPC technique. For example, the accuracy and precision with which structural information for polymers with broad molecular weight distribution, especially with long-chain branches, can be obtained depends critically on the accurate estimation of such calibration curves in the tails.

Traditionally, calibration curves are fit to the logarithm of the ratios of detector responses. However, the logarithm of a ratio will not give meaningful values in the regions where at least one of the responses is near zero. Thus, low detector sensitivity in the tails requires that a calibration curve be fit only to the heart of the peak, where all detectors have good response. The optimized

curve is then extrapolated to the regions in the tails that were excluded from the fit.

This data truncation has two consequences that limit the accuracy and precision of the multi-detector GPC technique. Truncation eliminates potentially useful responses with which to constrain the calibration curves, and the resulting curves can be sensitive to the choice of the fitting region.

We describe a new data analysis method for multi-detector GPC where the complete chromatographic profile obtained from one detector is compared, in a least-squares sense, to a model that is a function of responses from the other detector. This formulation of least-squares avoids the use of logarithms, ratios, and eliminates the need for extrapolation. The approach allows the inclusion of regions in the least-squares fit that contain low detector's signal, e.g., near baseline responses that fluctuate about zero from either, or both, detectors.

We apply this approach to obtain column calibration curves with each of two molecular weight-sensitive detectors, coupled to a GPC system. Such calibration curves are the necessary intermediate steps in determining the polymer's molecular weight and intrinsic viscosity distributions. If suitable calibration standards are available, we further show how the polymer's intrinsic viscosity law can be obtained directly from dual-detector responses without requiring - or depending on - a sample-dependent calibration curve.

INTRODUCTION

Multi-detector GPC is a powerful technique that can simultaneously characterize a wide range of a polymer's molecular properties. A conventional GPC system usually incorporates a single concentration detector, such as differential refractive index (DRI) detector. A multi-detector GPC system adds one or more molecular weight-sensitive detectors, typically a capillary viscometer (CV) and/or a static laser light-scattering photometer (LS). In conventional GPC, the determination of the absolute (actual) molecular weight and molecular weight distribution (MWD) of a polymer sample requires the use of polymer standards with chemical structure identical to the sample to calibrate the column. Dual-detector DRI-CV allows column calibration with standards having a different chemical structure than the sample. Dual-detector DRI-LS can calibrate the column using the sample itself, thereby, determining the MWD without the need of special calibrators.

There are additional benefits from the use of molecular weight-sensitive detectors. These include an improved characterization of high molecular weight fractions of the MWD, the ability to calculate molecular parameters such as the intrinsic viscosity distribution (IVD), the Mark-Houwink coefficients, the branching frequency across the polymer distribution, and the polymer conformation plot.

The price to pay for these benefits is the increased complexity of the data calibration and interpretation in multi-detector GPC. Thus, processing these data requires accurate values for instrument calibration constants, sample concentration, injection volume, flow rate, and interdetector volume(s). An error in any of these values will bias the calculated MWD.[1] Although, the accurate determination of these parameters complicates the data reduction in multi-detector GPC compared with its conventional counterpart,[1] these additional requirements do not limit the potential of this approach to polymer characterization.

The real challenge in multi-detector GPC data treatment arises from the nature of the detectors' sensitivities: molecular weight-sensitive detectors have low response at the low molecular weight end of a polymer distribution, and concentration detectors have low sensitivity at the high molecular weight end of this distribution.[2] In general, the local (slice) intrinsic viscosity or molecular weight values calculated from the DRI-CV or DRI-LS detector combinations, respectively, show high noise levels at the ends of the molecular weight range of the sample. Consequently, number-average molecular weight of polymers with low-molecular weight tail calculated with the use of molecular weight-sensitive detectors usually exceeds the true value; these values can be obtained more accurately with the concentration detector alone.

On the other hand, the accuracy of molecular weight distribution and other structural information about polymers with high-molecular weight tails, especially with long-chain branches, is limited by the sensitivity level of the concentration detector. However, this information is very important, for example, in determination of viscoelastic properties of polymer melts, such as dynamic moduli and steady-state recoverable compliance. These properties are extremely sensitive to minute variations in the high molecular weight tail of a polymer MWD,[3-5] which makes the microscopic approach to melt rheology in some cases more appropriate than GPC technique for evaluating molecular distributions of such polymers.[6]

The proper choice of data analysis methodology is the key to solving the aforementioned sensitivity problems in multi-detector GPC. In some cases, a least-squares fit of column calibration curve (molecular weight or intrinsic viscosity versus elution volume) to the heart of a peak, followed by model extrapolation, is an effective way to decrease the undesirable effect of high noise lev-

els at both ends of the polymer distribution.[7] But this approach requires the arbitrary truncation of the data region to exclude regions where signal-to-noise ratio is low. This exclusion adversely affects the results of calculation by excluding data that are potentially useful.

Additionally, the model for any calibration curve depends on the chromatographic system rather than on the polymer sample itself. The necessity to fit this curve with some empirical polynomial model, and then use the coefficients of this polynomial to calculate the values of the polymer parameters, also systematically biases the results.

We present advances in the treatment of data obtained from the multi-detection GPC of polymers with broad, and especially, tailed molecular weight distributions.

The first advance is in the method of least-squares fitting. We illustrate this method through its application to both molecular weight-sensitive detectors: LS and CV. This advance allows for the inclusion of data obtained from the tails of the polymer distribution in the estimation of calibration curves. We then describe a new approach to the problem of determining an intrinsic viscosity law (intrinsic viscosity versus molecular weight) from the multi-detector GPC measurements which circumvents the need to estimate calibration curves from sample data. Finally, we analyze some intrinsic viscosity laws based on the specific models of polymer branching (e.g., random long-chain branching),[8] and show how this model can be applied to the analysis of dual-detector measurements to obtain estimates of the branching properties of polymers.

These advances in the analysis of multi-detector GPC measurements, as applied to DRI-CV data, have been implemented in Millennium®[32] chromatography software package, Version 3.0 and later (Waters Corporation, Milford, MA, USA).[9] We demonstrate their experimental verification and their advantages as compared to traditional methods of analysis. Elsewhere,[10,i1] we discuss other ideas which can be applied to multi-detection GPC data reduction.

EXPERIMENTAL

All high temperature GPC experiments were performed with a new integrated Alliance GPCV 2000 system (Waters Corporation) incorporating DRI and differential CV detectors.[12] A set of three 10 μm Waters Styragel columns (7.8 mm I.D. × 300 mm) was used for size-exclusion separation: two HT 6E mixed bed linear columns with effective MW range $5\times10^3 - 10^7$ g/mol, and one HT 2 with effective MW range $10^2 - 10^4$ g/mol.

Twelve polystyrene narrow standards (Waters Corporation) between 2,630 and 4,480,000 g/mol molecular weights were used to create the universal cali-

bration curve (logarithm of hydrodynamic volume versus elution volume). The experimental points were fitted by a cubic polynomial. The eluent and solvent for all polyethylene and polystyrene samples was 1,2,4-trichlorobenzene (J. T. Baker, Phillipsburg, NJ, USA) filtered and dried with silica. The solvent for polymer solutions was stabilized with 0.017% Santonox-R (Monsanto Chemical Co., USA).

Two polyethylene standards (NIST 1475 and NIST 1476) were purchased from National Institute of Standards and Technology, Gaithersburg, MD, USA, and low-density polyethylene synthesized with metallocene catalysts – from Montell Polyolefins, Wilmington, Delaware.

The operating temperature of the column, detector, and injector compartments was 150°C. The injection volume was 0.3 mL and the flow rate was 1.00 mL/min. Data acquisition was performed with the Graphical User Interface (GUI) of Alliance GPCV 2000, data reduction was carried out with Millennium® ver. 2.15 (Figures 1 and 2), and Millennium®32 (Figures 3 and 4) (Waters Corporation).

RESULTS AND DISCUSSION

Relationship of Physical Properties to Detector Measurements

A differential refractometer measures the refractive index change , which is proportional to polymer concentration *C*, where

$$C = \frac{\Delta N}{\nu}, \tag{1}$$

and where ν = dn/dc, the refractive index increment of the polymer. An online capillary viscometer measures the pressure drop across a capillary tube over that of the pure solvent, which leads to the specific viscosity of a polymer solution.

Coupling these two detectors allows one to calculate the intrinsic viscosity, where

$$[\eta] \equiv \frac{\eta_{sp}}{C} = \frac{\eta_{sp}}{\Delta N}\nu . \tag{2}$$

If the hydrodynamic volume *H* for the polymer is known from the universal calibration curve, the polymer molecular weight M can then be calculated from the relationship:

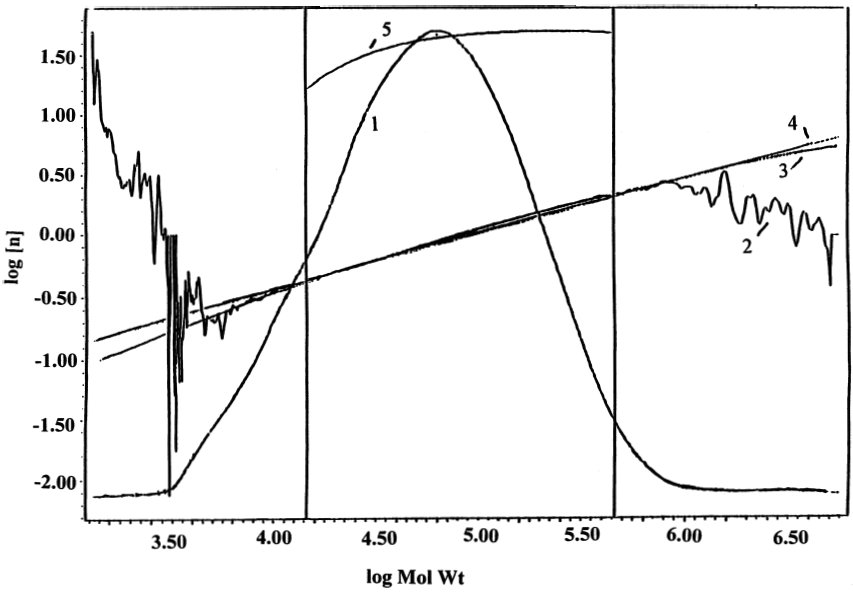

Figure 1. Sensitivity of intrinsic viscosity law to a choice of "good data region" in traditional approach. The molecular weight distribution and intrinsic viscosity law are plotted for NIST 1476 low-density polyethylene sample: (1) MWD; (2) observed intrinsic viscosity, $[\eta]_{obs}$; (3) fitted intrinsic viscosity, $[\eta]_{fit}$; (4) linear intrinsic viscosity, $[\eta]_{lin}$; (5) branching index, g'. "Good data region": log M_{min} = 4.16, log M_{max} = 5.67. Calculations are performed with Millennium 2.15, GPCV option (see text for details).

$$M \equiv \frac{H}{[\eta]} = \frac{\Delta N}{\eta_{sp}} \frac{H}{\nu}. \quad (3)$$

The intensity of the light scattered by a polymer solution at any given angle θ with respect to the forward direction, above that scattered by the pure solvent, is proportional to the excess Rayleigh ratio R_θ. The most important quantity for polymer applications is the excess Rayleigh ratio at zero angle R_0, which is provided directly by a low-angle laser light-scattering detector. Multi-angle light scattering (MALS) data need to be extrapolated to zero angle to obtain the value of R_0. For DRI-LS detection, the polymer molecular weight is calculated using formula

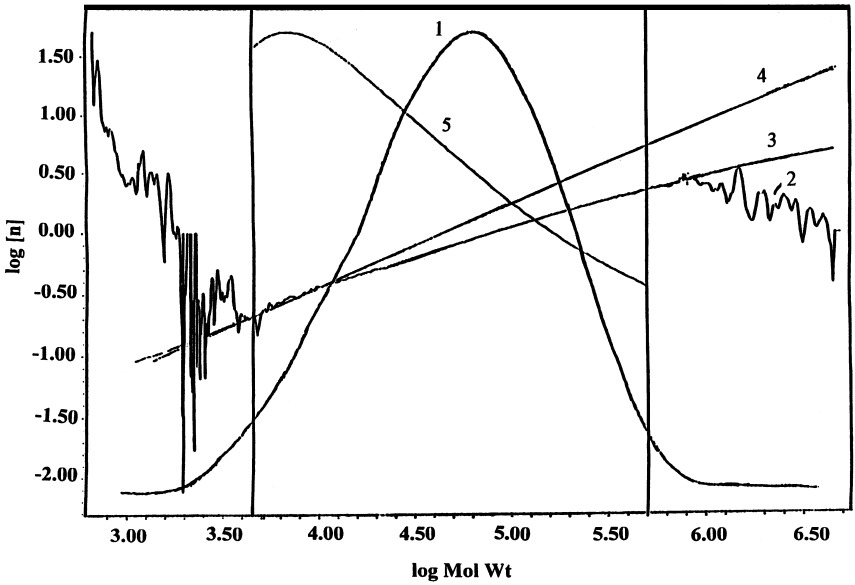

Figure 2. The same calculations as at Figure 1 with the exception of "good data region": log M_{min} = 3.65, log M_{max} = 5.70.

$$M = \frac{R_0}{K_{LS} C v^2} = \frac{R_0}{\Delta N} \frac{1}{K_{LS} v} \tag{4}$$

where $K_{LS} = 4\pi^2 n_0^2 / (\lambda_0^4 N_A)$, n_0 = refractive index of the solvent, λ_0 = wavelength of the incident light in a vacuum, N_A = Avogadro's number. A more general Rayleigh scattering law includes an additional dependence on the second virial coefficient. Our method applies either to this simpler or to the more complete expression.

If the universal calibration curve is available, one can still estimate the intrinsic viscosity from the DRI-LS detector combination, where

$$[\eta] \equiv H/M = \frac{\Delta N}{R_0} H K_{LS} v \tag{5}$$

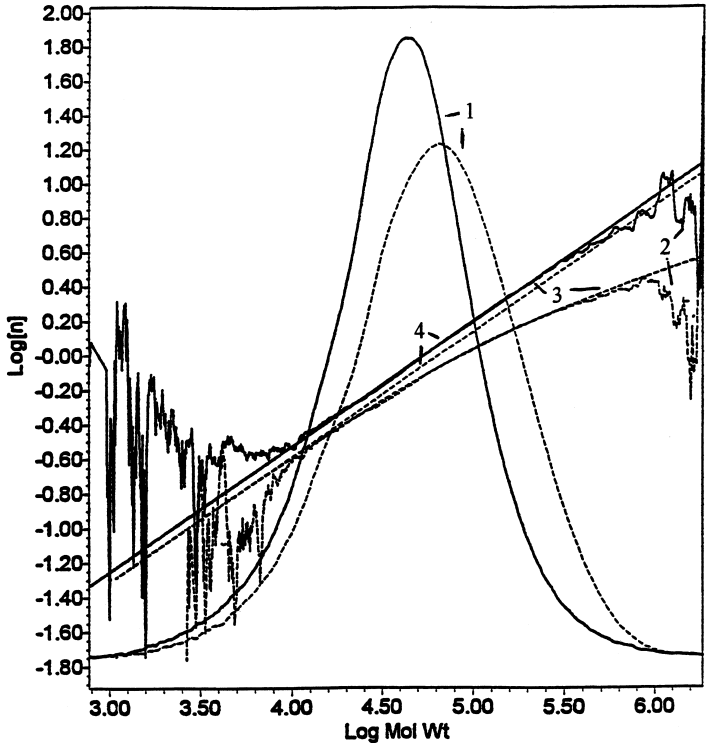

Figure 3. Molecular weight distributions and intrinsic viscosity law plots for NIST 1475 high-density polyethylene (solid lines) and NIST 1476 low-density polyethylene (dashed lines). The NIST 1475 data were fitted with Mark-Houwink equation (18) and the NIST 1476 data were fitted with the model (26) for randomly branched polymers. The curves' designations are the same as in Figure 1. Calculations are performed with new Millennium®[32], GPCV option (see the text for details).

Thus, either dual-detector combination can provide the polymer MWD, which is given by the normalized C versus log M, intrinsic viscosity distribution (C versus log [η]) and the intrinsic viscosity law, which is given by log [η] versus log M. For DRI-CV detection, equations (1), (2), and (3) are used to compute these values for each data point (slice) across the peak region. For the DRI-LS combination, equations (1), (4), and (5) are used to compute the slice values.

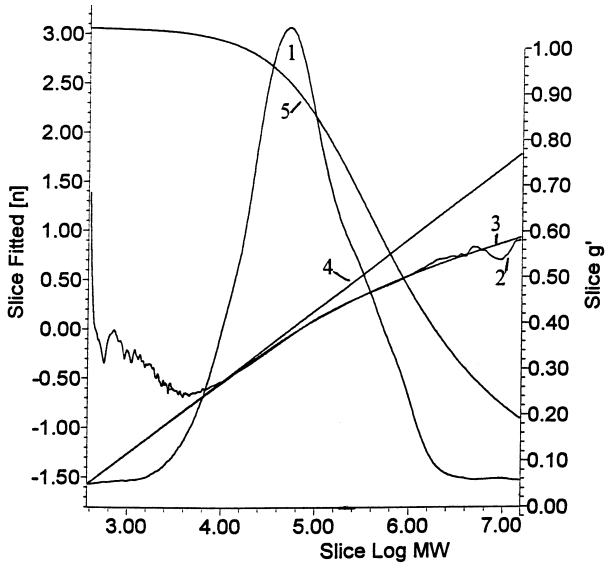

	Sample	Mn	Mw	Polydisp	g'	K	alpha	lambda
1	LDPE	26450	270944	10.24	0.571	0.000370	0.724	0.0000313

Figure 4. The Millennium®32 GPCV report on low-density polyethylene sample. Random branching model (26) was used for the intrinsic viscosity law fitting. The curves' designations are the same as in Figure 1. The linear intrinsic viscosity $[\eta]_{lin}$ (line (4)) is the asymptote to the $[\eta]_{fit}$ in the low molecular weight limit.

Triple-detector combination DRI-CV-LS eliminates the necessity to use universal calibration to calculate both molecular weight and intrinsic viscosity for each data point. Thus, equations (1), (2), and (4) allow for calculation of slice values.[11]

Effect of Detector Noise on Slice Measurements

Additive detector noise, seen as random fluctuations in the baseline having zero mean and a well-defined standard deviation, is an irreducible component

of the measurement process. As can be seen from equations (2)-(5), the molecular weights and intrinsic viscosities for each slice are proportional to the ratios of detector responses. It follows that detector noise introduces noise in quantities that depend on these ratios.

At the tails of the distribution, these ratios do not produce physically meaningful values. For example, values of molecular weight and intrinsic viscosity computed from slice ratios sometimes will not decrease monotonically with increasing elution volume. Thus, curves 2 in Figures 1-4 represent logarithm of intrinsic viscosity log $[\eta]_{obs}$ calculated from the DRI-CV detector combination as the ratio of two detector responses (equation (2)). The dramatic noise increase can be seen on both tails of the polymer distribution.

Fitting a smooth, multi-variate model to a time series of noisy data is generally an effective way to produce a more precise estimate of the measured quantity at each sample time. For the multi-detector combinations we are considering, the logarithm of the ratios,

$$\log[\eta]_i = \log\left(\frac{\nu\eta_{sp,i}}{\Delta N_i}\right) \tag{6}$$

$$\log M_i = \log\left(\frac{R_{0,i}}{K_{LS}\nu\Delta N_i}\right) \tag{7}$$

both tend to be nearly linear functions of elution volume. The calculations are accomplished by fitting a smooth parameterized model to these ratios as a function of slice number *i* or elution volume V_i, i.e., the total volume of eluent that has passed through the columns up to some specific time t_i. Thus, a low-order polynomial, as a function of elution volume, is an appropriate empirical model that can be fit to these quantities. Such polynomials then describe intrinsic viscosity and molecular weight calibration curves, respectively.

Typically, a linear least-squares procedure is used to fit a polynomial to the data. In some cases, when data points tend to scatter non-randomly around the fitted line, cubic splines are found to be a better choice for fitting.[13,14] In the following discussion we will focus only on the least-squares fitting of a model to data.

In performing a least-squares fit, equations (6) and (7) raise multiple difficulties near the tails of broad distributions. The effect of the logarithm in regions of low detector response is to increase the noise in log M and log [η], affecting measurements in the both tails of the peak. The negligibly small

response of the refractometer in the denominator of equations (6) and (7) gives rise to additional noise in log M and log [η] at the high-molecular-weight tail of the distribution. At the very ends of the peak tails, slice values of molecular weight and intrinsic viscosity will not decrease monotonically with increasing elution volume, and the noise in the responses can cause the ratios to have negative values. The logarithm of a negative number is not defined. This issue of dealing with the logarithm of the response ratios is described recently,[15] however, the authors proposed no solution to the problem.

Traditional Approach to Least-Squares Fitting

The usual assumption is that in peak tails, the quantities described in equations (6) and (7), because they appear dominated by noise, contain no useful information, and their inclusion would compromise the accuracy of a model fit. Least-squares fitting of models is then confined to the "heart" of the peaks where the signal-to-noise ratios for these quantities are high. This truncation is followed by the extrapolation of the model results to the polymer tails. Though critical to obtain the MWD for the entire polymer distribution, the extrapolation procedure is problematic. The results are extremely sensitive to the choice of the demarcation between the heart and tails of the peak (i.e., selection of so-called "good data region") and to the method of its implementation,[15,16] especially for polymers with tailed distributions.

For example, Figures 1 and 2 represent the results of quantitation of raw data collected for highly branched, low-density broad polyethylene standard NIST 1476. The set of two chromatograms (refractometer and viscometer, respectively) was treated using equations (1) - (3) with the universal calibration curve obtained with a set of narrow polystyrene standards. The fitted intrinsic viscosity (log $[\eta]_{fit}$) plot (curve 3) is obtained using a second-order polynomial fit to data inside the "good data region" indicated by the vertical lines and then extrapolated outside this region. The linear intrinsic viscosity (log $[\eta]_{lin}$) plot (curve 4) is described by a straight line fitted to the first 25% of polymer distribution beginning with the start of the "good data region". This line represents a Mark-Houwink plot for the linear low-molecular weight portion of this polymer.

The ratio $g' = [\eta]_{fit} / [\eta]_{lin}$ calculated for each data point (curve 5) is the branching index (branching contraction factor), which quantitatively characterizes the degree of long-chain branching in every polymer fraction. This quantity should decrease monotonically with molecular weight for polymers with long-chain branches. The only difference between Figures 1 and 2 is the selection of the "good data region." One can see a dramatic difference in intrinsic viscosity law plots and branching information (i.e., branching index plot) caused by this selection.

Given that the measurement errors in $\log[\eta]_i = \log\left(\frac{v\eta_{sp,i}}{\Delta N_i}\right)$ and $\log M_i = \log\left(\frac{R_{0,i}}{K_{LS}v\Delta N_i}\right)$ differ significantly from slice to slice, can estimates obtained from a fitting model be made more precise by the inclusion of weight functions in each term in the least-squares fit?[13,14] Weighting will allow in the inclusion of data from a broader region, as data near the tails will be weighted to have less significance than data near the heart of the peak.

However, to yield optimum results, the weight function must accurately reflect the errors in the terms of any model polynomial function. When any of the values ΔN, R_0, or η_{sp} becomes comparable to the magnitude of detector noise (e.g., in the peak tails), weighting, as implemented in,[13,14] is limited by three factors:

Due to the non-linear nature of the logarithm, the errors in the terms of a polynomial induced by detector noise are asymmetrical with respect to their true values. Weighting does not account for asymmetrical errors.

The errors in these terms are highly sensitive functions of the true values for ΔN, R_0, or η_{sp}. This makes it essentially impossible for a weight to be meaningfully computed in the peak tails, where the errors are fractionally large.

Weighting does not allow the inclusion of slice data whose values result in the logarithm of a negative argument.

Though weighting can be incorporated into the traditional formulation of least-squares, it will still require an arbitrary truncation of the data region and will not reflect the asymmetrical errors that the logarithms produce.

New Approach to Molecular Weight Calibration Curve Fitting

We illustrate the new approach[17] to least-squares fitting by first applying it to the determination of the calibration curve in DRI-LS detection. This curve is typically assumed to be a polynomial describing as a function of an *N*th order polynomial in V. Thus the model to be fit is

$$F_M \equiv \log M_{fit} = C_0 + C_1V + C_2V^2 + \cdots + C_NV^N \qquad (8)$$

where F_M is a function of V and the fitting parameters $C_0, \cdots C_N$. Note that the parameters $C_0, \cdots, C_N$ describing the calibration curve depend on both poly-

mer structure and separation system including chromatographic conditions (columns, mobile phase, and temperature).

In the traditional application of least-squares, the values for the parameters $C_0, \cdots, C_N$ are obtained by finding those parameters that minimize the following expression

$$S^2 = \sum_{i=1}^{L} \left(\log M_i - F_{M,i} \right)^2 \tag{9}$$

In this expression, the values for $\log M_i$ are the molecular weight estimates obtained from the slice measurements using equation (7). The values $F_{M,i}$ are the model values for $\log M_{fit}$ at each slice i, and the sum is over the entire data region (L slices). Thus, the least-squares fit compares the model values $F_{M,i}$ to a combination of data involving the logarithm of a ratio of measurements. As described above, the error in the slice estimates, $\log M_i$, varies across the polymer distribution and approaches infinity as the signal approaches zero, near the baseline. It is this unbounded increase in error that requires that the fitting region be truncated.

Our new approach to least-squares fitting uses the same model, equation (8), for the calibration curve, but directly compares the measurements of R_0 to a *model* of R_0. The quantity to be minimized is then

$$S^2 = \sum_{i=1}^{L} \left(R_{0,i} - \Delta N_i K_{LS} \nu 10^{F_{M,i}} \right)^2 \tag{10}$$

Equation (10) compares the measured, excess Raleigh ratio $R_{0,i}$, determined by light-scattering detection, to a model of that value. Following equation (4), the model is the product of the refractometer response ΔN_i, optical constant K_{LS}, refractive index increment ν, and the molecular weight M_i for this slice, as given by the model of the calibration curve, $10^{F_{M,i}}$, from equation (8).

Equation (10) is a rearrangement of the same quantities used in equation (9). However, there are important advantages to this rearrangement. Because the errors in $R_{0,i}$ and ΔN_i are assumed to have zero mean and distributed as Gaussian, the error in each residual term, $R_{0,i} - \Delta N K_{LS} \nu 10^{F_{M,i}}$, will also have zero mean and be distributed as a Gaussian. Thus, all the chromatographic profile data in the fit can be used, including points for which the measured values for ΔN_i and $R_{0,i}$ are consistent with zero and in fact have negative values due to noise. The above expression, thus, can be used to fit for data throughout the peak region, including the tails.

Further, equation (10) takes advantage of the fact that regions containing zero signal still provide useful information to constrain the least-squares fit. Thus, in the low-molecular weight region the light-scattering signal may be negligible, yet this region can be included in the sum in equation (10).

Further Optimization Using Weighted Least-Squares

An estimation method is optimum if it yields parameters whose estimates are unbiased and have minimum possible variance for a given level of detector noise.[18] Even though equation (10) will produce a more precise and accurate estimate of the calibration curve than will equation (9), we can still ask: does equation (10) represent an *optimum* solution to the problem of estimating a calibration curve from DRI-LS data?

Fitting a multi-variate curve to data containing noise is a common problem in the statistical analysis of data. Maximum likelihood estimation yields optimum estimates of parameters in multi-variate models.[18] It describes how to find parameter values that are unbiased and have minimum sensitivity to the noise in the data. Thus, if a set of experimental data d_i is compared with the model values $D_i=D_i(C_1,\cdots,C_N)$, then the optimum (least-sensitive to noise) estimates of the parameters $C_1,\cdots,C_N$ is obtained by finding those parameter values that minimize the following expression:

$$\chi^2 = \sum_{i=1}^{L} \frac{(d_i - D_i)^2}{\sigma_i^2} \tag{11}$$

Here each squared difference between measured d_i and model D_i values is weighted by the square of the standard deviation σ_i.

To obtain correct parameter estimates (i.e., the correct calibration curve), only the relative noise values are important. For example, if all the terms have the same noise variance, then setting $\sigma_i = 1$ for all terms (unweighted least-squares) will still yield the correct values for the parameters.

According to theory[18,19] the estimation procedures based on weighted least-squares fitting (11) are generally optimum if the noise in quantities d_i is additive, has zero mean, is unbiased, and described by a distribution having standard deviation σ_i.

The noise properties of the refractometer, light scattering or viscometer detectors correspond to the most common type of instrumental noise and possess all aforementioned properties. Thus, the optimum estimate of the calibration curve is obtained from the weighted-least-squares generalization of equation (10), which is

$$\chi^2 = \sum_{i=1}^{L} \frac{\left(R_{0,i} - \Delta N_i K_{LS} v 10^{F_{M,i}}\right)^2}{\sigma_i^2}, \quad (12)$$

where σ_i^2 is the variance of the quantity in the numerator $(R_{0,i} - \Delta N_i K_{LS} v 10^{F_{M,i}})$. The appropriate variance is

$$\sigma_i^2 = \sigma_{LS}^2 + \sigma_{RI}^2 (K_{LS} v 10^{R_i})^2, \quad (13)$$

where σ_{LS}^2 and σ_{RI}^2 are the variances of the baseline noise associated with the respective detectors, light scattering and refractive index.

In principle, equations (12) and (13) are an improvement over equation (10). But is that a significant improvement in practice? If $\sigma_{LS}^2 \gg \sigma_{RI}^2 (K_{LS} v 10^{R_i})^2$ for each slice (which is possible if the light-scattering detector is noisier than the refractive index detector), then the variance in each term of equation (10) is a constant over the peak region. Unweighted least-squares is than an appropriate approach, and equation (10) yields an optimum estimate of the calibration curve.

In order for least squares fitting to be implemented, an algorithm must be used to find the parameters $C_0, \cdots, C_N$ that minimize S^2. As for any minimization procedure, the final values for these parameters will not depend on the details of the algorithm adopted to perform the minimization, as long as the minimum is actually found. In general, such minimization procedures require that initial parameters values be found and that an initial value for S^2 be computed. Theses parameters are then iteratively adjusted by a variety of standard methods such as Newton-Raphson, Levenberg-Marquadt, simplex, gradient search, and brute force search.[19]

New Approach to Intrinsic Viscosity Calibration Curve Fitting

In the previous section, we described the new approach to least-squares fitting to determine the molecular weight calibration curve from the LS detector. The same approach can be used in determination of the intrinsic viscosity calibration curve from the viscometer detection. In DRI-CV combination, the intrinsic viscosity is typically modeled as an *N*th order polynomial in elution volume V. Thus, the model to be fit is

$$F_{[\eta]} \equiv \log[\eta]_{fit} = C_0 + C_1 V + C_2 V^2 + \cdots + C_N V^N, \quad (14)$$

where $F_{[\eta]}$ is a function of V and the fitting parameters $C_0, \cdots, C_N$.

In the standard application of least-squares, the values for the parameters are obtained by minimizing following expression

$$S^2 = \sum_{i=1}^{L} \left(\log[\eta]_i - F_{[\eta],i} \right)^2 \tag{15}$$

In this expression, the values for $\log[\eta]_i$ are the intrinsic viscosity estimates obtained from the slice measurements using equation (6). The values $F_{[\eta],i}$ are the model values for $\log[\eta]_{fit}$ at each slice i, and the sum is over L slices. Again, the least-squares fit compares a model to the logarithm of a ratio of measurements. The error in the slice estimates, $\log[\eta]_i$, varies across the polymer distribution and approaches infinity as the signal approaches zero, near the baseline.

As in the case of the DRI-LS analysis, the new approach to least-squares fitting for DRI-CV analysis compares a measurement to a model. The least-squares problem then takes on the following form:

$$S^2 = \sum_{i=1}^{L} \left(\eta_{sp,i} - 10^{F_{[\eta],i}} \frac{\Delta N_i}{\nu} \right)^2 \tag{16}$$

where $\eta_{sp,i}$ is the measurement of specific viscosity. The quantity $10^{F_{[\eta],i}} \frac{\Delta N_i}{\nu}$ is the model of specific viscosity.

The advantages of equation (16) are the same as for equation (10). The noise in the quantity $\left(\eta_{sp,i} - 10^{F_{[\eta],i}} \frac{\Delta N_i}{\nu} \right)$ is nearly constant over the whole peak profile. In contrast, the noise in the quantity $(\log[\eta]_i - F_{[\eta],i})$ is unstable in the peak tails. Again, equation (16) can be used to determine the intrinsic viscosity of a distribution throughout the whole peak region - in the heart of the peak and in the peak tails. This equation allows one to obtain $\log[\eta]$ as a polynomial expansion in elution volume, thereby, arriving at the smooth intrinsic viscosity calibration curve (14).

Calculation of Polymer's Distributions

Constructing the smooth molecular weight (8) and intrinsic viscosity (14) calibration curves are important intermediate steps in determining the polymer's molecular weight and intrinsic viscosity distributions. If both curves (8)

and (14) are constructed from the triple detector combination (DRI-CV-LS), then given the values for C, $\log[\eta]_{fit}$, and $\log M_{fit}$ for each slice, one estimates both polymer's distributions. If only a single molecular weight-sensitive detector is coupled to a GPC system, then the smooth hydrodynamic volume (universal) calibration curve (log H versus V) may replace that calibration curve, which is unavailable due to the absence of the appropriate detector. This can be achieved via the relation $\log H = \log M_{fit} + \log[\eta]_{fit}$.

The hydrodynamic volume calibration curve can be obtained for both dual detection combinations from a set of polymer standards with narrow polydispersity. In the case of the DRI-CV combination, the peak molecular weight for each standard is to be known prior to the calculations, while for the DRI-LS system the Mark-Houwink constants make it possible to construct the universal calibration.

New Method for Estimating Intrinsic Viscosity Law

While the MWD and IVD are important characteristics of any polymer sample, they still do not provide information about molecular structure of macromolecules, e.g., their architecture. This information can be obtained from the intrinsic viscosity law (IVL), log [η] versus log M. We can represent a model for the IVL as

$$[\eta] = [\eta(C_0,C_1,...,C_N;M)] \tag{17}$$

where $C_0,C_1,...,C_N$ are the parameters that specify the distribution's intrinsic viscosity as a function of molecular weight M. For example, the empirical Mark-Houwink relationship is given by

$$[\eta(K,\alpha;M)] \equiv KM^{\alpha} \tag{18}$$

where $C_0 = K$ and $C_1 = \alpha$. Any IVL is the inherent property of polymer sample in dilute solution. This means that its parameters $C_0,C_1,...,C_N$ depend on molecular structure of polymer only, and not on the properties of a chromatographic system, e.g., the column set.

The model for IVL can be constructed through the additional fit from any pair of calibration curves (molecular weight, intrinsic viscosity, and hydrodynamic volume). Thus, as triple detector data could obtain the two calibration curves, $\log[\eta]_{fit}$ versus V and $\log M_{fit}$ versus V, for the sample, then one could eliminate V to obtain $\log[\eta]_{fit}$ versus for each slice. A model of the form $[\eta] = [\eta(C_0,C_1,...,C_N;M)]$ could be fit to these values to determine the parameters $C_0,C_1,...,C_N$.

We have seen how dual-detector DRI-LS data can obtain the log M_{fit} versus V calibration curve for the polymer distribution. With the addition of a suitable set of polymer standards and the assumption of universal calibration, DRI-LS data can also determine the $\log[\eta]_{fit}$ versus V curve for this sample, and thus the sample's IVL.

We will now describe in detail two ways that a distribution's IVL can be obtained from DRI-LS data. In the first way, one obtains log M_{fit} versus V via application of equation (10) to the DRI-LS data obtained from the sample. One next measures the molecular weight for the calibrators from the DRI-LS data obtained from their respective peaks. These molecular weights combined with the prior knowledge of the calibrator's Mark-Houwink constants yields the column's hydrodynamic calibration, log $H(V)$. This determination requires that a model curve, such as a low-order polynomial, be fit to the log H versus V values obtained from each calibrator. Finally, the value for $\log[\eta]_{fit}$ for each slice follows from the definition $\log[\eta]_{fit} = \log H - \log M_{fit}$.

The method just described has a significant limitation. The accuracy of the IVL depends on the accuracy of the sample-dependent calibration curve: $\log[\eta]_{fit}$ versus V. Inaccuracy in this model will adversely affect the determination of the polymer's IVL. For example, even for a polymer with strictly linear configuration described by linear Mark-Houwink equation, $\log[\eta]_{fit}$ versus V will generally be a non-linear function of elution volume V.

We now demonstrate a new method for determining the IVL that eliminates the need to determine this empirical calibration curve. The key to the method is to use the hydrodynamic calibration to re-express the IVL as a function of elution volume. This is done in three steps, as follows.

Given a model expression $[\eta]=[\eta(C_0,C_1,...,C_N; M)]$, we first obtain its inverse, $M=M(C_0,C_1,...,C_N;[\eta])$. We then combine this with the definition of hydrodynamic volume H, $H = M[\eta]$, to eliminate M. We now have a model for the intrinsic viscosity as a function of H, as follow:

$$[\eta] = [\eta(C_0,C_1,...,C_N;H)] \tag{19}$$

In the case of the Mark-Houwink relationship, the inversion can be accomplished algebraically to yield $M_i = ([\eta]_i/K)^{1/\alpha}$, and the elimination of the dependence on M yields the desired form of the IVL:

$$[\eta]_i = H_i^{1/(1+\alpha)} K^{\alpha/(1+\alpha)}, \tag{20}$$

These two steps are purely algebraic manipulations that can be applied to any IVL. For more complex forms of IVLs, numerical inversion will be needed to express the IVL in the form of equation (19).

The third step uses the column calibration obtained from the standards, log *H (V)* to eliminate *H* in equation (19), leading to the parameterized model

$$[\eta_i] = [\eta(C_0,C_1,...,C_N;V_i)] \tag{21}$$

Equation (21) describes [η] as a function of *V*, parameterized by the structural parameters $C_0,C_1,...,C_N$, and not by an empirical form such as equation (14). The interpretation of equation (21) is straightforward. Each slice can be regarded as a separate experiment that has the potential to constrain the distribution parameters $C_0,C_1,...,C_N$.

Given the formulation of the IVL as expressed in equation (21), we can find the values for the$C_0,C_1,...,C_N$ that minimize

$$S^2 = \sum_{i=1}^{L}\left(R_{0,i} - \Delta N_i K_{LS} v \frac{H(V_i)}{[\eta(C_0,C_1,\ldots,C_N;V_i)]}\right)^2 \tag{22}$$

Note that the calibration curve, log $[\eta]_{fit}$ versus V, is automatically obtained as part of the determination of the IVL. Again, equation (22) has the advantage that the errors in $R_{0,i} - \Delta N_i K_{LS} v \frac{H(V_i)}{[\eta(C_0,C_1,\ldots,C_N;V_i)]}$ are symmetrical and finite for all slice values, and data at the baseline can be included.

The analysis of dual-detector DRI-CV data parallels that of DRI-LS data. We have seen how dual-detector DRI-CV can obtain the log $[\eta]_{fit}$ versus *V* calibration curve. With the addition of a suitable set of polymer standards and the assumption of universal calibration, DRI-CV data can also determine log M_{fit} versus *V*, and thus the sample's IVL.

Again, we can take two paths. In the first way, one obtains log $[\eta]_{fit}$ versus *V* via application of equation (16) to the DRI-CV data from the sample. One next measures the intrinsic viscosity for the calibrators from the DRI-LS data. Combined with the prior knowledge of the calibrator's molecular weights, and a suitable model for hydrodynamic calibration curve, these intrinsic viscosities yield log *H* (*V*). Finally, the value for log $M_{fit}(V)$ for each slice follows from the definition log M_{fit} (V) = log H(V)−log $[\eta]_{fit}$(V).

The new method for determining the IVL again employs the log *H (V)* obtained from the standards, so we can again express the IVL in the form given by equation (20). We then obtain values for $C_0,C_1,...,C_N$ by optimizing

$$S^2 = \sum_{i=1}^{L} \left(\eta_{sp,i} - [\eta(C_0, C_1, \ldots, C_N; V_i)] \frac{\Delta N_i}{\nu} \right)^2 \quad (23)$$

with respect to these parameters. Again, this new formulation expresses the IVL in terms of the structural parameters and not the ones that describe column properties.

Application to Linear Polymers

For the empirical Mark-Houwink relationship, we can substitute equation (20) into equation (23) and obtain

$$S^2 = \sum_{i=1}^{L} \left(\eta_{sp,i} - H_i^{1/(1+\alpha)} K^{\alpha/(1+\alpha)} \frac{\Delta N_i}{\nu} \right)^2 \quad (24)$$

which is the least-squares problem whose solution gives values of K and α. The model value of $[\eta]_i$ for each slice i is then obtained from equation (20), and the polymer molecular weight for this slice is calculated from the relationship $M_i = (H_i/K)^{1/(1+\alpha)}$.

In this proposed formulation, the model of the intrinsic viscosity law is found without introducing an unneeded model that describes the elution of the sample from the chromatographic columns. In equation (24), the column enters in only through the hydrodynamic volume calibration curve as determined from the standards. The parameters describing the intrinsic viscosity law are then determined directly from the sample's detector responses. Again, in equation (24), the errors in $\eta_{sp,i} - H_i^{1/(1+\alpha)} K^{\alpha/(1+\alpha)} \Delta N_i/\nu$ are symmetrical and finite for all slice values, and data at the baseline can be included.

Application to Branched Polymers

The intrinsic viscosity law across the whole polymer peak region provides important information about the molecular structure of a branched polymer. This information is especially important at its high-molecular-weight tail, where even a slight deviation from the linear Mark-Houwink equation can indicate significant change in macromolecular structure. The opportunity to construct this plot from the GPC data is a significant benefit of any multi-detection system.

Our new approach generalizes to any intrinsic viscosity law of the form (17). For intrinsic viscosity laws more complex then the Mark-Houwink equation, a simple algebraic inversion may not suffice to determine $[\eta]$ as a function

of H in closed form. A numerical method for inverting the equation[19] may be employed as part of the minimization procedure.

In the case of a linear polymer, two Mark-Houwink coefficients K and α are enough to account for the intrinsic viscosity law across the whole polymer distribution. A polymer with short-chain branches can also be described by Mark-Houwink equation with the same exponent α as its linear counterpart, but with lower value of parameter K.[20,21] A more complex model is needed to account for the intrinsic viscosity law for long-chain branched polymers. The Zimm-Stockmayer model describes the ratio g of mean-square radii of gyration of polymers with and without random long-chain branches.[22] Combined with semi-empirical relations of the form[8] $g' = g^{\varepsilon}$, this model yields the following equation for macromolecules with molecular weight M

$$[\eta] = [\eta]_{\text{lin}} \left(\lambda M / c_1 + \sqrt{1+\lambda M / c_2}\right)^{-\frac{\varepsilon}{2}}, \tag{25}$$

where $c_1 = 9\pi/4$, $c_2 = 7$ for the three-branch point and $c_1 = 3\pi/4$, $c_2 = 6$ for the four-branch point; $[\eta]_{\text{lin}}$ describes the intrinsic viscosity of the polymer backbone without long-chain branching; λ is the chain branching frequency (branching probability per Dalton), i.e., the number of branching points divided by molecular weight of polymer chains, and ε is the shape (or structural) factor which varies between 1/2 and 3/2.[8] The randomness of branching means the molecular weight independence of λ, which constitutes the main assumption behind the model.[22] Using the Mark-Houwink relationship for $[\eta]_{\text{lin}}$, we obtain the intrinsic viscosity law for randomly branched polymers:

$$\log[\eta] = \log K + \alpha \log M - \frac{\varepsilon}{2} \log\left(\lambda M / c_1 + \sqrt{1+\lambda M / c_2}\right), \tag{26}$$

which is applied for each slice i of a polymer distribution.

As can be seen from equation (26), intrinsic viscosity is described by four parameters, K, α, ε, and λ. According to this model, the polymer is essentially unbranched at low molecular weight side, and its intrinsic viscosity law is asymptotically linear in this region and described by Mark-Houwink constants, K and α. This linear intrinsic viscosity plot is denoted curve 4 in Figures 3 and 4.

Recall that the presence of short-chain branches can be indicated by the value of parameter K. The accuracy of determination of these two parameters is affected dramatically by the low molecular weight portion of the chromatograms. This is why the inclusion of this region in the least-squares fit is so important.

At extremely high molecular weight, when branching dominates, the asymptotic slope of the intrinsic viscosity law is less than α, and is given by $\alpha-\varepsilon/2$. This region exists in highly branched polymers only. The intermediate region is affected mostly by the value of branching density λ. This portion of the chromatograms usually corresponds to high molecular weight fractions of typical branched polymers, where the response of the concentration detector is close to the noise level. Again, the inclusion of this region is very important for the accuracy of calculations.

More complex models for branched polymers may require empirical models, such as given by the polynomial expansion:

$$\log [\eta] = \log K + \alpha_1 \log M + \alpha_2 \log^2 M + \cdots + \alpha_N \log^N M \qquad (27)$$

In Millennium®32 the determination of a polymer's intrinsic viscosity law and molecular weight distribution can be obtained for either:

Mark-Houwink law, via application of equation (20),

Model for polymers with random long-chain branches, via the application of equation (26), or

Polynomial model, via the application of equation (27). The polynomial model for intrinsic viscosity is supported up to fifth order in log *M*.

Calculation of the Intrinsic Viscosity Law for Polyethylene Samples

The detailed analysis of branched polymers based on the foregoing approach is to be published soon.[21] In what follows, we present just a few examples for the purposes of illustration. Figure 3 demonstrates the results obtained with new approach (16), (21) for two NIST broad polyethylene standards: high-density linear polyethylene NIST 1475 and branched low-density polyethylene NIST 1476 (the raw GPC data for the last one are the same as that of Figures 1 and 2). The Mark-Houwink model (18) was used to process data for linear NIST 1475 sample, while the randomly branched polymer model (24) (three-branch point) was employed for branched NIST 1476 polyethylene.

Practically the same values of Mark-Houwink exponent α was found for both polymers (0.7261 for NIST 1475 and 0.7275 for NIST 1476), which almost coincide with reported[20] value 0.725 for these polymers obtained at slightly lower temperature (TCB, 135°C). At the same time, the values of *K* for these two polymers are significantly different: 0.371×10^{-3} and 0.320×10^{-3}, respectively (see the difference between the solid and dashed lines 4 in Figure 3). This difference is far beyond the reproducibility limit of the calculation and can be attributed to short-chain branches in NIST 1476, obtained in free-radical polymerization.

This important information about polymer structure becomes available through the novel algorithm just described. This approach allows the inclusion of regions that contain no signal caused by the polymer in solution in the least-squares fit, e.g., baseline responses that fluctuate about zero from either, or both, detectors. This makes the results much less sensitive to integration and considerably improves the accuracy of the measured sample's MWD and intrinsic viscosity law obtained with multi-detection GPC.

Note that the model (26) appeared to be suitable for variety of polyethylenes with long-chain branches. Thus, Figure 4 represents the calculated multimodal MWD and intrinsic viscosity law curves for low-density polyethylene, synthesized with the mixture of two single-site metallocene catalysts, producing a polymer with long-chain branching. In spite of apparent complexity of the molecular structure, the model (26) with four physical parameters K, α, ε, and λ fits the observed intrinsic viscosity throughout the entire polymer distribution. Note that K value obtained (0.37×10^{-3}) is the same as that of NIST 1475, which unequivocally indicates the absence of short-chain branches in the polymer under investigation.

CONCLUSION

Significant expansion of polymer characterization capabilities of GPC centers around on-line molecular-weight-sensitive detectors coupled to a concentration detector. This multi-detector approach offers great advantages in the accurate characterization of complex polymers, provided that results based on ratios of measured signals are interpreted properly. A novel method of fitting multi-detector data to obtain more accurate MWD and intrinsic viscosity law was derived. A chromatographic profile obtained from one detector is compared, in a least-squares sense, to a model that is a function of responses from another detector.

This model for optimization represents the appropriate calibration curve (molecular weight or intrinsic viscosity) or the intrinsic viscosity law and is used to fit measured chromatographic profiles. The intrinsic viscosity law can be described by Mark-Houwink relation for linear polymers; the randomly branched polymer model for polymers with long-chain branching, empirical low-order polynomials, etc. This formulation of least-squares significantly improves the accuracy of the measured sample's MWD and other structural characteristics obtained with multi-detector GPC.

REFERENCES

1. T. H. Mourey, S. T. Balke, "A Strategy for Interpreting Multi-detector Size-Exclusion Chromatography Data I," in **Chromatography of Polymers:**

Characterization by SEC and FFF, ACS Symposium Series, T. Provder, ed., Washington, DC, 1993, pp. 180-198.

2. C. Jackson, H. G. Barth, "Molecular Weight-Sensitive Detectors for Size Exclusion Chromatography," in **Handbook of Size Exclusion Chromatography**, Chi-san Wu, ed., Chromatographic Science Series, Vol. 69, J. Cazes, ed., Marcel Dekker, Inc., New York, 1995, pp. 103-145.

3. G. Eder, H. Janeschitz-Kriegl, S. Liedauer, A. Schausberger, W. Stadlbauer, G. Schindlauer, J. Rheol., **33**, 805-820 (1989).

4. J. P. Montfort, G. Marin, Ph. Monge, Macromolecules, **17**, 1551-1562 (1984).

5. B. H. Bersted, J. Appl. Polym. Sci., **30**, 3751-3765 (1985).

6. D. Becker, A. Franck, D. Mead, American Lab., **30**, 18-20 (1998).

7. C.-Y. Kuo, T. Provder M. E. Koehler, A. F. Kah, "Use of a Viscometric Detector for Size Exclusion Chromatography," in **Detection and Data Analysis in Size Exclusion Chromatography,** ACS Symposium Series, Vol. 352, T. Provder, ed., Washington, DC, 1987, pp. 130-154.

8. A. Rudin, "Measurement of Long-Chain Branch Frequency in Synthetic Polymers," in **Modern Methods of Polymer Characterization,** H. G. Barth, J. W. Mays, eds., John Wiley & Sons, 1991, pp. 103-112.

9. Y. Brun, M. Gorenstein, N. Hay, R. Nielson, "New Results in Polymer Characterization Using Multi-detector GPC," in **Proceedings, International GPC Symposium,** Phoenix, Arizona, 1998, pp.48-67.

10. Y. Brun, "Triple Detection in SEC: New Potentials for Polymer Characterization," in **Proceedings, International GPC Symposium,** San Diego, CA, 1996, pp. 116-153.

11. Y. Brun, J. Liq. Chrom. & Rel. Technol., **21**, 1979-2015 (1998).

12. Y. Brun, R. Nielson, "Polyolefin Characterization Using a New Integrated GPC System," in **Proceedings, International GPC Symposium,** Phoenix, Arizona, 1998, pp.415-436.

13. P. Cheung, S. T. Balke, T. H. Mourey, J. Liq. Chromatogr., **15**, 39 (1992).

14. S. T. Balke, P. Cheung, L. Jeng, R. Lew, J. Appl. Polym. Sci. Appl. Polym. Symp., **48**, 259 (1991).

15. P. Tackx, F. Fosscher, Anal. Comm., **34**, 295-297 (1997).

16. R. Lew, P. Cheung, S. T. Balke, T. H. Mourey, J. Appl. Polym. Sci., **47**, 1685-1700 (1993).

17. M. V. Gorenstein, Y. Brun, Patent Pending, 1997.

18. B. P. Martin, **Statistics for Physicists**, Academic Press, NY, 1971, pp. 85-98.

19. W. H. Press, S. A. Teukolsky, W. T. Vetterling, B. P. Flannery, **Numerical Recipes in C, the Art of Scientific Computing**, 2nd Ed., Univ. of Cambridge, 1992, pp. 394-455.

20. T. G. Scholte, N. L. J. Meijerink, H. M. Schoffeleers, A. M. G. Brands, J. Appl. Polym. Sci., **29**, 3763-3782 (1984).

21. Y. Brun, M. V. Gorenstein, in preparation.

22. B. H. Zimm, W. H. Stockmayer, J. Chem. Phys., **17**, 1301-1314 (1949).

Received April 12, 2000
Accepted May 4, 2000

Author's Revisions June 6, 2000
Manuscript 5282